

NU  
S82/v

March · Vol. 85 · DP17644

# steel research

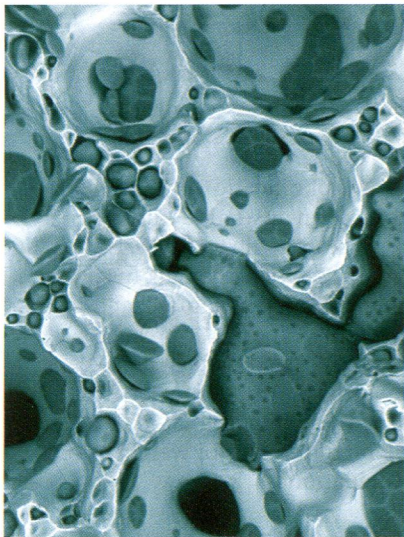
international

3  
2014

[www.steel-research.de](http://www.steel-research.de)

WILEY-VCH





# steel research

international



www.steel-research.de

## Cover Photo:

Steel matrix syntactic foams are fascinating materials with great development potential. Their properties include low weight, a metal foam-like response to compressive load and a strength levels exceeding other steel foams. The wide range of matrix/filler combinations possible will allow their fine-tuning to application requirements once structure-property relationships are fully understood. The image shows the fracture surface of a powder metallurgical 316L foam containing 5 wt.-% of glass microspheres, see the article by Dirk Lehmhus and co-workers. Unlike cenospheres, the glass microspheres disintegrate during processing, resulting in a glass phase (medium gray phase, light gray: 316L matrix) embedded in between matrix grains and at inner surface of pores. The latter mark the original position of the microspheres.

## Publishing company:

Wiley-VCH Verlag GmbH & Co. KGaA,  
Boschstraße 12, D-69469 Weinheim,  
Germany

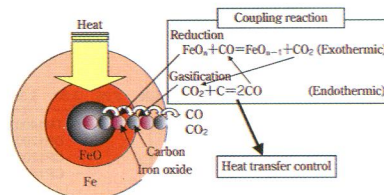
## Contents

### Review Article

H. M. Ahmed,\* N. Viswanathan and  
B. Bjorkman

### Composite Pellets – A Potential Raw Material for Iron-Making

293



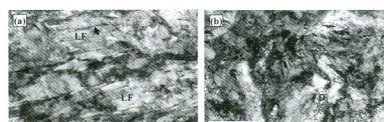
Using carbon composite pellets as a raw material for iron making processes has the great potential as it can derive the following advantages simultaneously: (i) Replacing expensive coke with relatively less expensive carbon sources, (ii) Producing agglomerates from cheaper raw materials, and (iii) Making the process towards higher carbon utilization. However, they also pose challenges in terms of strength and making the reactions happen at desired conditions. A review on these aspects has been presented here.

### Full Paper

D.-Z. Li,\* Y.-C. Liu, T.-X. Cui, J.-M. Li,  
Y.-T. Wang and P.-M. Fu

### The Effect of Thermo-Mechanical Processing Parameters on Micro- structure and Mechanical Properties of a Low Carbon, High Strength Steel

307



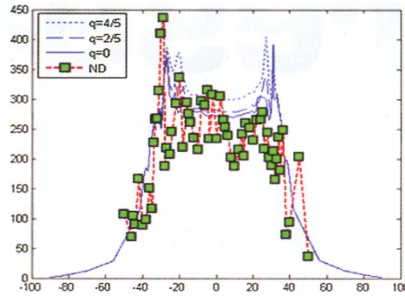
The morphology of carbon-free bainite ferrites BFs and remained austenite films which are located between them and acicular ferrite containing dislocation are presented in figure a. The morphology of martensite M and dislocations D in acicular ferrite are indicated in figure b.

# Contents

K. Decroos,\* C. Ohms, R. Petrov,  
M. Seefeldt, E. Verhaeghe and  
L. Kestens

## Influence of Texture on Welding Stress Calculations

314

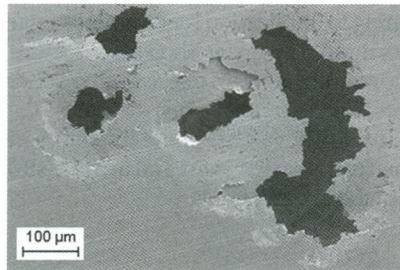


Upon solidification of the fusion zone of an austenitic weld a strong crystallographic texture arises. As a consequence, the bulk fusion zone material becomes transversely isotropic. This paper presents a procedure to define an anisotropic material law for the fusion zone, and to implement that in Finite Element models for welding stress calculations.

H. Pulkkinen,\* H. Apajalahti, S. Papula,  
J. Talonen and H. Hänninen

## Pitting Corrosion Resistance of Mn- Alloyed Austenitic Stainless Steels

324

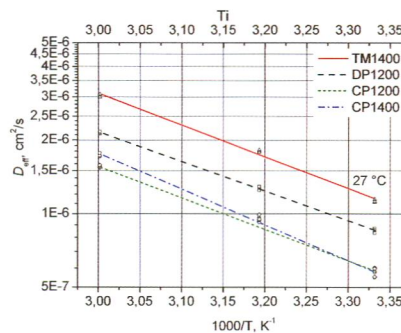


The role of composition, inclusions and precipitates on the pitting corrosion resistance of Mn-alloyed austenitic stainless steels is examined. The Mn-sulfides are observed to act as corrosion pit initiators in chloride containing solutions. As the Cr content is decreased and Ni partially replaced by Mn the pitting corrosion resistance is reduced.

J. Rehr,\* K. Mraczek, A. Pichler and  
E. Werner

## The Impact of Nb, Ti, Zr, B, V, and Mo on the Hydrogen Diffusion in Four Different AHSS/UHSS Microstructures

336



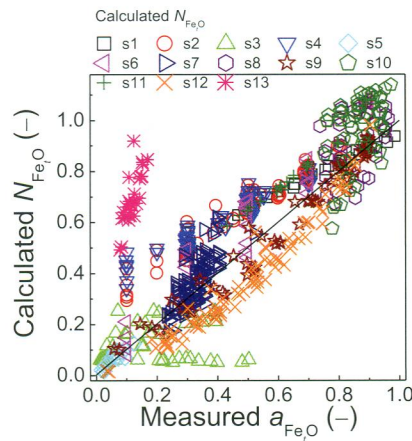
In this work hydrogen diffusion in four non- and microalloyed AHSS/UHSS grades has been investigated. The results indicate that hydrogen diffusion depends significantly on the microstructure adjusted. The tempered martensitic grade shows the highest diffusivity, followed by the dual-phase steel. Complex-phase steel grades reveal the lowest diffusivity. However, precipitates and substitutional atoms of microalloying elements seem to have a negligible effect on hydrogen diffusion.

# Contents

X.-M. Yang,\* M. Zhang, J.-L. Zhang,  
P.-C. Li, J.-Y. Li and J. Zhang

## Representation of Oxidation Ability for Metallurgical Slags Based on the Ion and Molecule Coexistence Theory

347

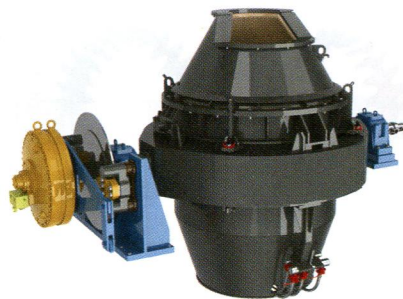


To calculate the defined comprehensive mass action concentration  $N_{\text{FeO}}$  of iron oxides in the selected slag systems, a thermodynamic model for calculating the mass action concentrations of structural units or ion couples in CaO–SiO<sub>2</sub>–MgO–FeO–Fe<sub>2</sub>O<sub>3</sub>–MnO–Al<sub>2</sub>O<sub>3</sub>–P<sub>2</sub>O<sub>5</sub> type slags, i.e., the IMCT- $N_i$  model, has been developed. The cover shows the reliable agreement between the calculated comprehensive mass action concentration  $N_{\text{FeO}}$  of iron oxides by the developed IMCT- $N_i$  model and reported activity  $a_{\text{FeO}}$  of iron oxides in 13 slag systems at different temperatures. The determined comprehensive mass action concentration  $N_{\text{FeO}}$  of iron oxides can be successfully applied to predict the oxidation ability of metallurgical slags.

A. Tilliander,\* L. T. I. Jonsson and  
P. G. Jönsson

## A Three-Dimensional Three-Phase Model of Gas Injection in AOD Con- verters

376

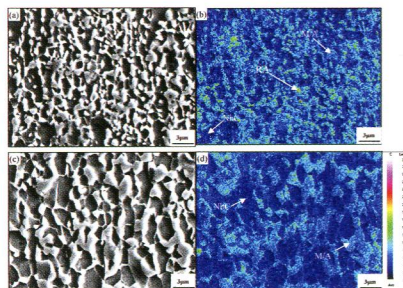


A 3D 3-phase (steel, slag and gas) AOD model with an industrial relevant geometry including six nozzles has been used to predict fluid flow, turbulence and bubble characteristics as well as fluid-slag dispersion. Also, two different gas flow rates have been simulated. This new findings opens up for further investigations of gas-metal reactions in the AOD converter.

C. Wang, H. Ding,\* Z. Tang, J. Zhang  
and H. Di

## The Effect of Intercritical Annealing on the Microstructure and Mechan- ical Properties in a High Strength TRIP Steel with C-Partitioning

388

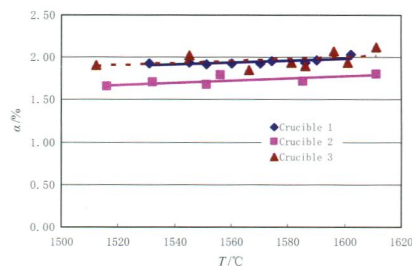


In this study, the effect of intercritical annealing on the microstructure and mechanical properties with C-partitioning is investigated for a high strength transformation-induced plasticity steel (TRIP steel). The partitioning of C to austenite during intercritical annealing are the main contributions to the austenite stability is confirmed by direct experimental evidence (WDS). After heat treatment, C atoms mainly exist among the granular retained austenite and the M/A islands.

# Contents

L. Zhong,\* M. Zeze and K. Mukai  
Density and Molar Volume of Liquid  
Iron Containing Nb

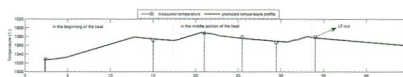
395



The linear expansion of the alumina crucibles used in this density measurement is about 1.65–2.07 at the temperature range from 1510 to 1610°C. The linear expansion increases linearly with an increase in temperature. Crucible 1 and 3 seem to have the same expansion coefficients, but crucible 2 has a lower expansion coefficient than those of crucible 1 and 3.

W. Lv, Z. Mao,\* P. Yuan and M. Jia  
Pruned Bagging Aggregated Hybrid  
Prediction Models for Forecasting the  
Steel Temperature in Ladle Furnace

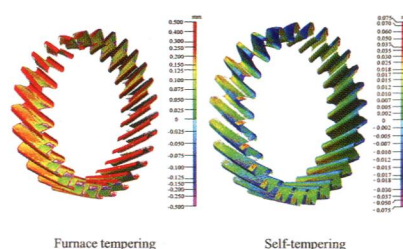
405



A novel prediction model is developed for real-time forecasting the steel temperature during LF refining process. In order to obtain good continuous prediction capability, a hybrid predictor is firstly developed by combining first principle method with data-driven modeling technique. Thereafter, a modified ensemble learning algorithm is introduced for further boosting prediction accuracy.

D. Rodman,\* F. Nürnberger, A. Dalinger,  
M. Schaper, C. Krause, M. Kästner and  
E. Reithmeier  
Tempering Induction Hardened  
42CrMo4 Steel Helical Gearwheels  
from Residual Heat Using Spray  
Cooling

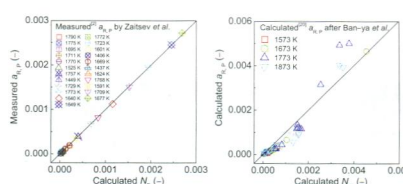
415



During induction hardening of helical gearwheels made of 42CrMo4 heat-treating steel using spray cooling, a self-tempering was performed. The result of the heat treatment is analyzed with the aid of hardness, residual stress, and distortion measurements. The obtained hardening results demonstrate the equivalence of self-tempering and conventional furnace tempering.

X.-M. Yang,\* P.-C. Li, J.-Y. Li, M. Zhang,  
J.-L. Zhang and J. Zhang  
Representation Reaction Abilities  
of Structural Units and Related  
Thermodynamic Properties in Fe–P  
Binary Melts Based on the Atom–  
Molecule Coexistence Theory

426



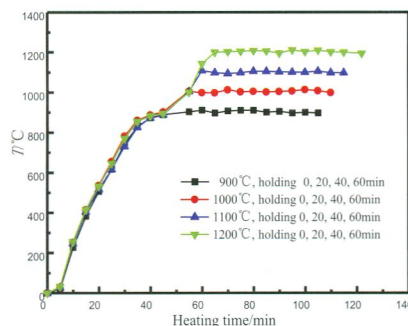
A thermodynamic model for calculating the mass action concentrations of structural units in Fe–P binary melts based on the atom–molecule coexistence theory, i.e., AMCT– $N_i$  model, has been developed and verified through comparing with the reported activities of both P and Fe in Fe–P binary melts with mole fraction  $x_p$  of P < 0.33 in a temperature from 1406 K to 1973 K. The cover shows that the calculated mass action concentration  $N_p$  of P can correlate a very good 1:1 corresponding relationship with the reported activity  $a_{R,P}$  of P relative to pure liquid P(l) as standard state.

# Contents

J.-j. Hao, J. Chen,\* P.-d. Han, K. Li and H.-f. Sun

## Solid Phase Decarburization Kinetics of High-Carbon Ferrochrome Powders in the Microwave Field

461

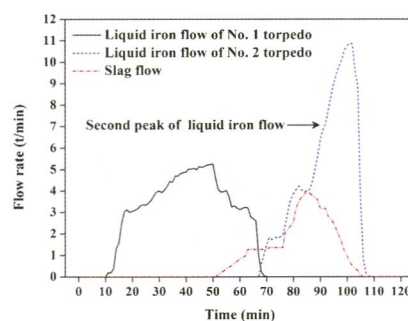


This paper deals with the kinetics of solid phase decarburization of HCFPs in microwave heating filed. Apparent activation energy of the solid phase decarburization reaction is calculated and restrictive step and the mechanism is also obtained. The optimum conditions of solid phase decarburization of HCFP by microwave heating are also concluded.

K. Du,\* S. Wu, M. Kou, W. Shen and Z. Zhang

## Numerical Simulation of Liquid Iron Flow and Heat Transfer in the Hearth of COREX Melter Gasifier during Tapping Process

466



In comparison with blast furnace, the second peak of liquid iron flow at the later stage of tapping, which mainly results from the expansion of taphole diameter, is a distinguishing feature of COREX melter gasifier hearth. The practical experience shows that depressurization tapping and improving the clay properties are effective measures to minimize the second peak of liquid iron flow.

A. Jahn, K.-P. Steinhoff, T. Dubberstein,\* P. Franke, M. Weider, S. Wolf, A. Kovalev, A. Glage, A. Weiß, W. Schärfl, K. Eigenfeld, L. Krüger and P. R. Scheller

## Phosphor Alloyed Cr–Mn–Ni Austenitic As-cast Stainless Steel with TRIP/TWIP Effect

477

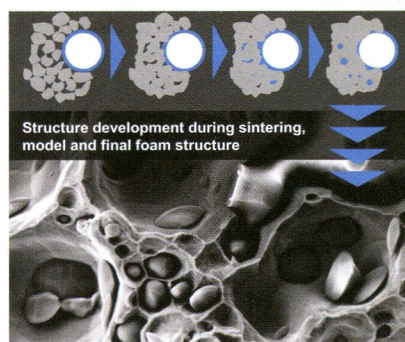


The influence of increasing phosphor content on the flowability, the effect on the infiltration of  $ZrO_2$  open foam ceramics, the martensite formation as well as the resulting mechanical properties and the surface tension of high alloyed Cr–Mn–Ni as-cast steels are studied. The elongation properties are not influenced by increasing phosphor content.

J. Weise, D. Lehnhus,\* J. Baumeister, R. Kun, M. Bayoumi and M. Busse

## Production and Properties of 316L Stainless Steel Cellular Materials and Syntactic Foams

486



316L steel matrix syntactic foams are produced via MIM and using soda-lime borosilicate hollow glass microspheres as filler. Structural development is evaluated using metallographic, image analysis and FIB preparation as well as EDX analysis techniques. Mechanical behavior is studied under quasi-static compressive and tensile load and qualitatively linked to structural features.